4. Shear strength of discontinuities

Introduction

All rock masses contain discontinuities such as bedding planes, joints, shear zones and faults. The failure of these rock masses involves failure of both the rock blocks, defined by intersecting discontinuities, and failure of the discontinuities. Failure of the individual intact rock blocks was discussed in the previous chapter on intact rock strength. This chapter is devoted to a discussion on the behaviour of the discontinuities.

Shear strength of planar surfaces

Assume that several samples of a rock are obtained for shear testing. Each sample contains a through-going bedding plane that is cemented; in other words, a tensile force would have to be applied to the two halves of the specimen to separate them. The bedding plane is planar, having no surface irregularities or undulations. As illustrated in Figure 1, in a shear test each specimen is subjected to a stress σ_n normal to the bedding plane and the shear stress τ required to cause a displacement δ.

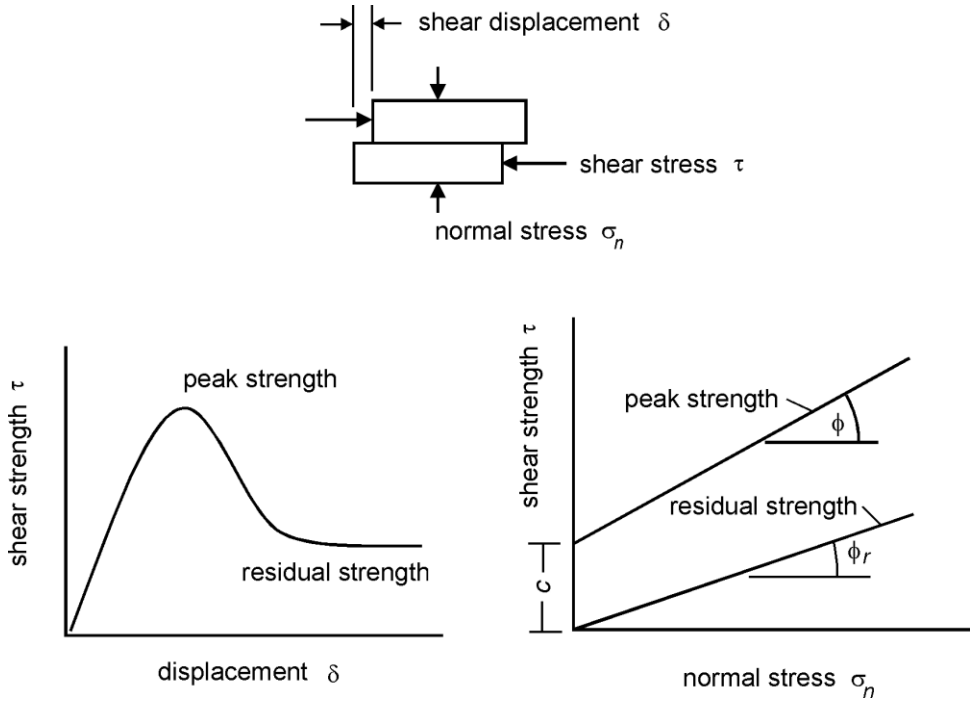

Figure 1: Shear testing of discontinuities.

The shear stress will increase rapidly until the peak strength is reached. This corresponds to the sum of the strength of the cementing material bonding the two halves of the bedding plane together and the frictional resistance of the matching surfaces. As the displacement continues, the shear stress will fall to some residual value that will then remain constant, even for large shear displacements. This residual strength depends on the frictional properties of the discontinuity surface.

Plotting the peak and residual shear strengths for different normal stresses results in the two lines illustrated in Figure 1. For planar discontinuity surfaces the experimental points will generally fall along straight lines. The peak strength line has a slope of ϕ and an intercept of c on the shear strength axis. The residual strength line has a slope of ϕ_r.

The relationship between the peak shear strength τ_p and the normal stress σ_n can be represented by the Mohr-Coulomb equation:

$$\tau_p = c + \sigma_n \tan\phi \qquad (1)$$

where c is the cohesive strength of the cemented surface and
ϕ is the angle of friction.

In the case of the residual strength, the cohesion c has dropped to zero and the relationship between ϕ_r and σ_n can be represented by:

$$\tau_r = \sigma_n \tan\phi_r \qquad (2)$$

where τ_r is the residual shear strength and
ϕ_r is the residual angle of friction.

A typical shear testing machine, which can be used to determine the friction angle ϕ is illustrated in Figures 2 and 3. This is a very simple machine. The use of a mechanical lever arm ensures that the normal load on the specimen remains constant throughout the test. This is an important practical consideration since it is difficult to maintain a constant normal load in hydraulically or pneumatically controlled systems which makes it difficult to interpret test data. Note it is important that, in setting up the specimen, great care must be taken to ensure that the shear surface is aligned accurately to avoid the need for an additional angle correction.

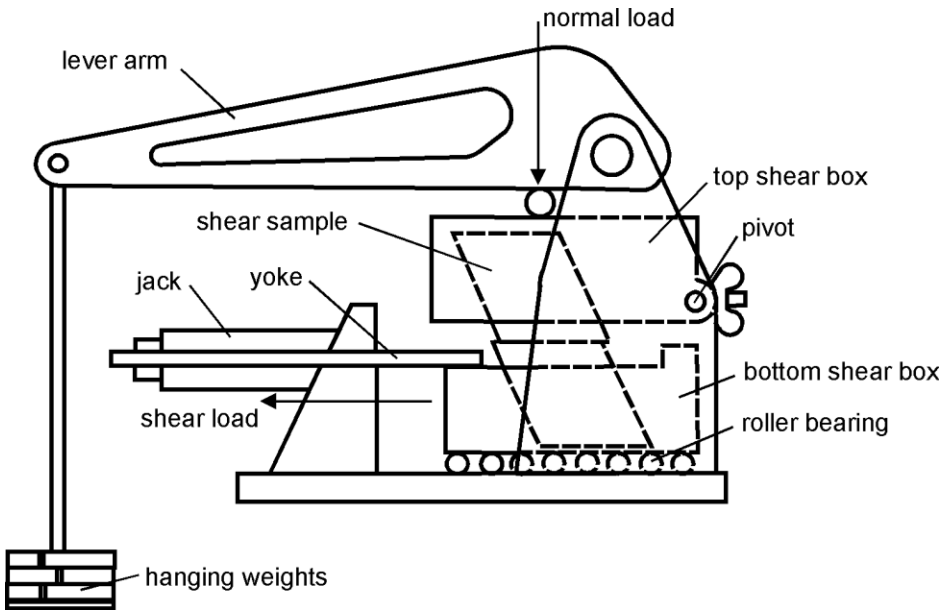

Figure 2: Diagrammatic section through shear machine used by Hencher and Richards (1982).

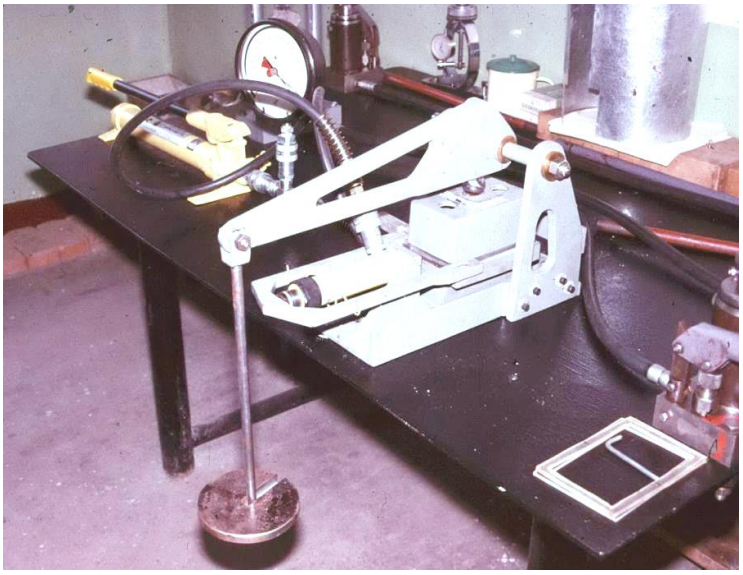

Figure 3: Shear machine of the type used by Hencher and Richards (1982) for measurement of the shear strength of sheet joints in Hong Kong granite.

Most shear strength determinations today are carried out by determining the basic friction angle, as described above, and then making corrections for surface roughness as discussed in the following sections of this chapter. In the past, there was more emphasis on testing full scale discontinuity surfaces, either in the laboratory, or in the field.

There are a significant number of papers in the literature of the 1960s and 1970s describing large and elaborate in situ shear tests, many of which were carried out to determine the shear strength of weak layers in dam foundations. However, the high cost of these tests together with the difficulty of interpreting the results, has resulted in a decline in the use of these large-scale tests. They are seldom seen today.

The author's opinion is that it makes both economical and practical sense to carry out a number of small scale laboratory shear tests, using equipment such as that illustrated in Figures 2 and 3, to determine the basic friction angle. The roughness component, which is then added to this basic friction angle to give the effective friction angle, is a number which is site specific and scale dependent and is best obtained by visual estimates in the field. Practical techniques for making these roughness angle estimates are described below.

Shear strength of rough surfaces

A natural discontinuity surface in hard rock is never as smooth as a sawn or ground surface of the type used for determining the basic friction angle. The undulations and asperities on a natural joint surface have a significant influence on its shear behaviour. Generally, this surface roughness increases the shear strength of the surface. This strength increase is extremely important in terms of the stability of excavations in rock.

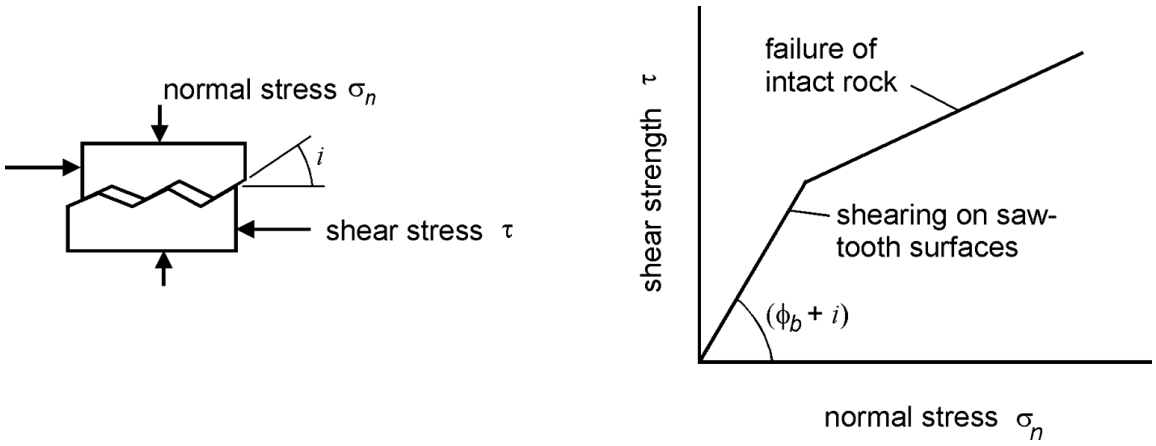

Figure 4: Patton's experiment on the shear strength of saw-tooth specimens.

Patton (1966) demonstrated this influence by means of an experiment in which he carried out shear tests on 'saw-tooth' specimens such as the one illustrated in Figure 4. Shear displacement in these specimens occurs because of the surfaces moving up the inclined faces, causing dilation (an increase in volume) of the specimen.

The shear strength of Patton's saw-tooth specimens can be represented by:

$$\tau = \sigma_n \tan(\phi_b + i) \tag{3}$$

where ϕ_b is the basic friction angle of the surface and
i is the angle of the saw-tooth face.

Equation (3) is valid at low normal stresses where shear displacement is due to sliding along the inclined surfaces. At higher normal stresses, the strength of the intact material will be exceeded, and the teeth will tend to break off, resulting in a shear strength behaviour which is more closely related to the intact material strength.

Barton's estimate of shear strength

While Patton's approach has the merit of being very simple, it does not reflect the reality that changes in shear strength, with increasing normal stress, is gradual rather than abrupt. Barton and Choubey (1977) studied the behaviour of natural rock joints and carried out direct shear test results on 130 samples of variably weathered rock joints. They proposed that equation 3 could be re-written as:

$$\tau = \sigma_n \tan\left(\phi_r + JRC \log_{10}\left(\frac{JCS}{\sigma_n}\right)\right) \tag{4}$$

Where ϕ_r is the residual friction angle
JRC is the joint roughness coefficient and
JCS is the joint wall compressive strength.

Barton and Choubey suggest that the residual friction angle ϕ_r can be estimated from

$$\phi_r = (\phi_b - 20) + 20(r / R) \tag{5}$$

where r is the Schmidt hammer rebound number for wet and weathered fracture surfaces and R is the Schmidt rebound number on dry unweathered sawn surfaces.

Equations 4 and 5 have become part of the Barton-Bandis criterion for rock joint strength and deformability (Barton and Bandis, 1990).

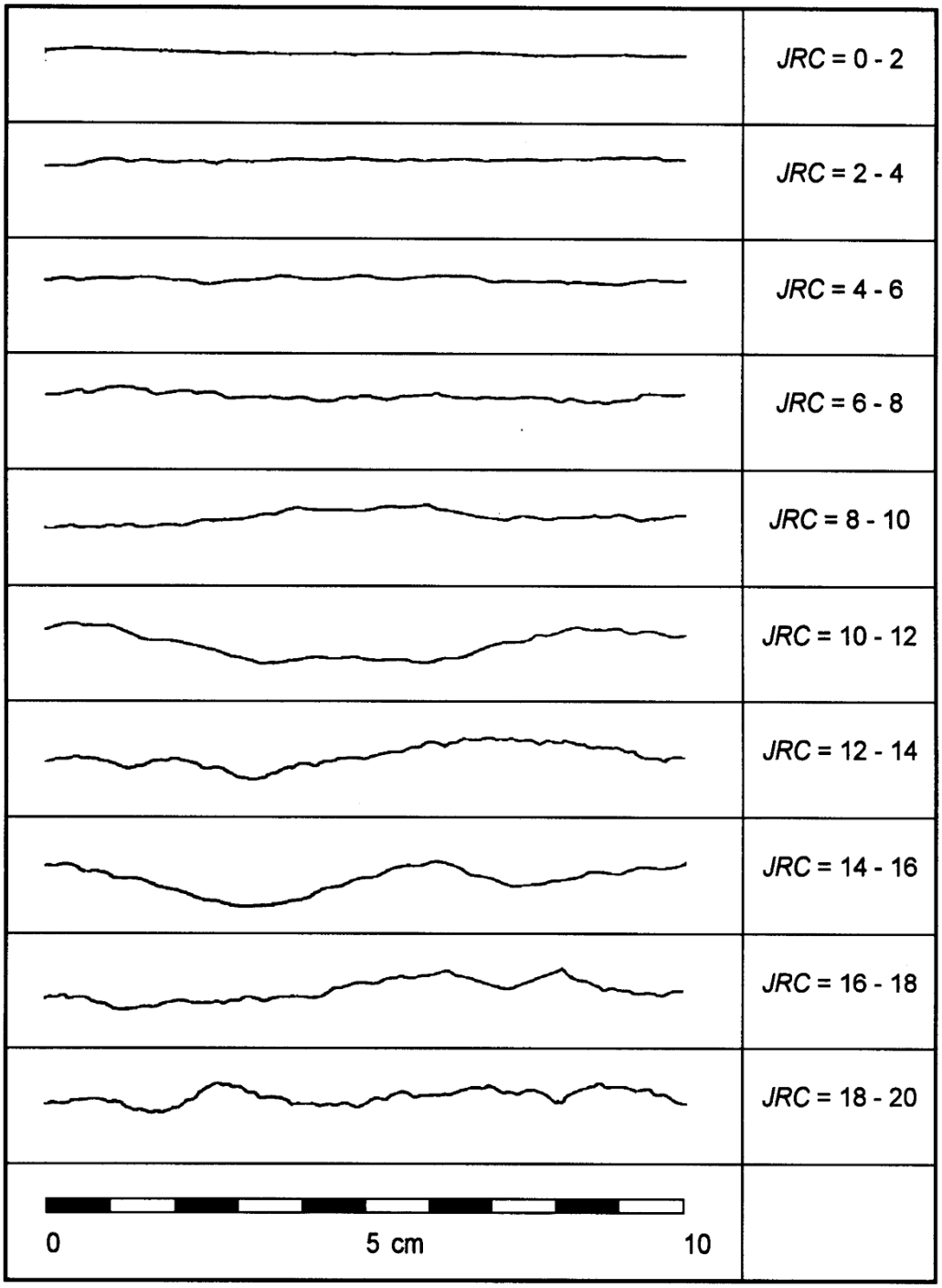

Figure 5: Roughness profiles and corresponding *JRC* values (After Barton and Choubey, 1977).

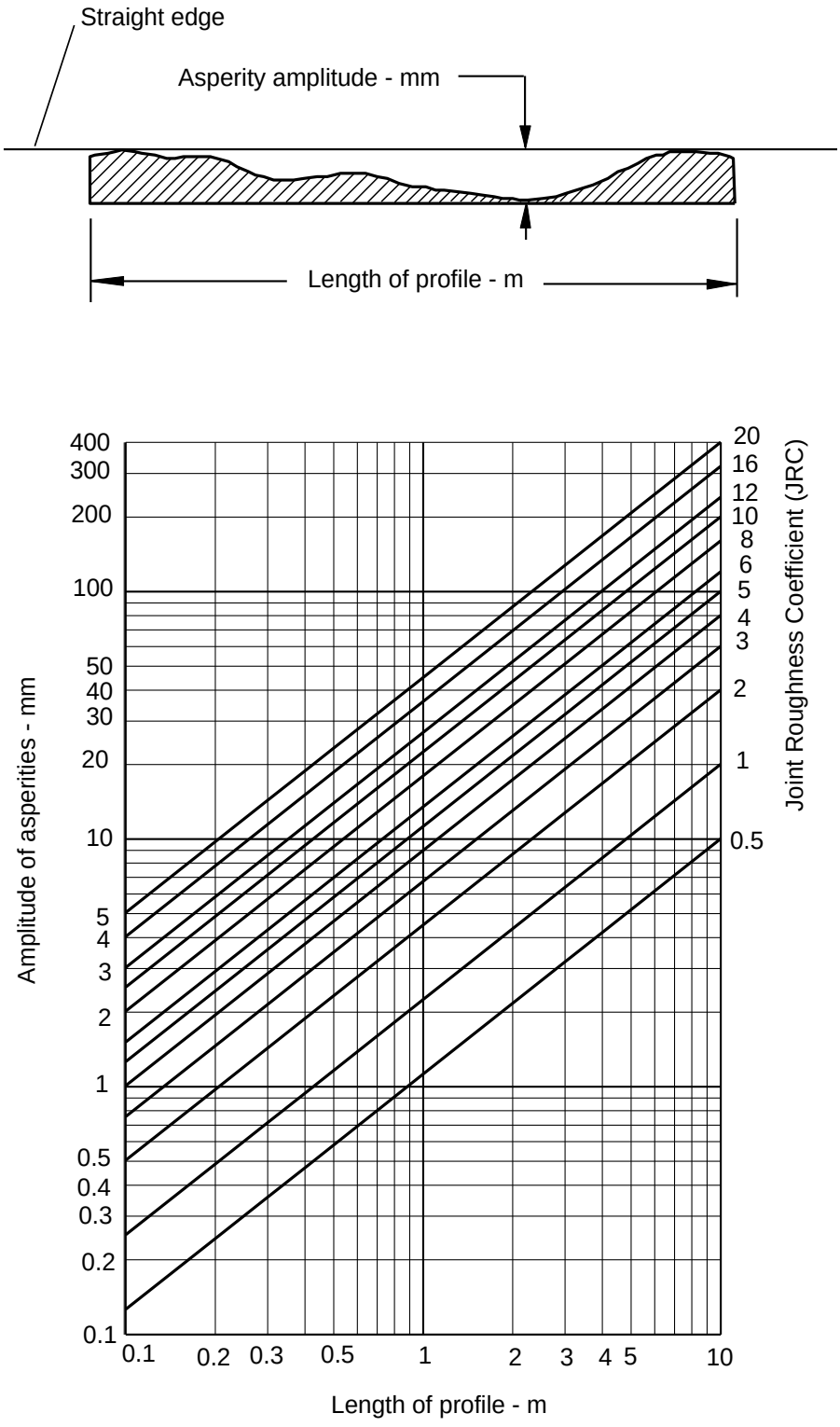

Figure 6: Alternative method for estimating *JRC* from measurements of surface roughness amplitude from a straight edge (Barton 1982).

Field estimates of *JRC*

The joint roughness coefficient *JRC* is a number that can be estimated by comparing the appearance of a discontinuity surface with standard profiles published by Barton and others. One of the most useful of these profile sets was published by Barton and Choubey (1977) which is reproduced in Figure 5.

The appearance of the discontinuity surface of the sample is compared visually with the profiles shown in Figure 5. The *JRC* value corresponding to the profile which most closely matches that of the discontinuity surface is chosen. In the case of small-scale laboratory specimens, the scale of the surface roughness will be approximately the same as that of the profiles illustrated. However, in the field the length of the surface of interest may be several metres or even tens of metres and the *JRC* value must be estimated for the full-scale surface.

An alternative method for estimating *JRC*, proposed by Barton (1982), is presented in Figure 6.

Influence of scale on *JRC* and *JCS*

Based on extensive testing of joints, joint replicas, and a review of literature, Barton and Bandis (1982) proposed a scale correction for *JRC* defined by the following relationship:

$$JRC_n = JRC_o \left(\frac{L_n}{L_o} \right)^{-0.02\,JRC_o} \tag{6}$$

where JRC_o, and L_o (length) refer to 100 mm laboratory scale samples and JRC_n, and L_n refer to in situ block sizes.

Because of the greater possibility of weaknesses in a large surface, it is likely that the average joint wall compressive strength (*JCS*) decreases with increasing scale. Barton and Bandis (1982) proposed the scale corrections for *JCS* defined by the following relationship:

$$JCS_n = JCS_o \left(\frac{L_n}{L_o} \right)^{-0.03\,JRC_o} \tag{7}$$

where JCS_o and L_o (length) refer to 100 mm laboratory scale samples and JCS_n and L_n refer to in situ block sizes.

Shear strength of filled discontinuities

The discussion presented in the previous sections has dealt with the shear strength of discontinuities in which rock wall contact occurs over the entire length of the surface under consideration. For planar surfaces, such as bedding planes in sedimentary rock, a thin clay coating will result in a significant shear strength reduction. For a rough or undulating joint, the filling thickness must be greater than the amplitude of the undulations before the shear strength is reduced to that of the filling material.

A comprehensive review of the shear strength of filled discontinuities was prepared by Barton (1974). A summary of the shear strengths of typical discontinuity fillings, based on Barton's review, is given in Table 1.

Table 1: Shear strength of filled discontinuities and filling materials (After Barton 1974).

Rock	Description	Peak c' (MPa)	Peak ϕ°	Residual c' (MPa)	Residual ϕ°
Basalt	Clayey basaltic breccia, wide variation from clay to basalt content	0.24	42		
Bentonite	Bentonite seam in chalk Thin layers Triaxial tests	0.015 0.09-0.12 0.06-0.1	7.5 12-17 9-13		
Bentonitic shale	Triaxial tests Direct shear tests	0-0.27	8.5-29	0.03	8.5
Clays	Over-consolidated, slips, joints and minor shears	0-0.18	12-18.5	0-0.003	10.5-16
Clay shale	Triaxial tests Stratification surfaces	0.06	32	0	19-25
Coal-measure rocks	Clay mylonite seams, 10 to 25 mm	0.012	16	0	11-11.5
Dolomite	Altered shale bed, ±150 mm thick	0.04	1(5)	0.02	17

Diorite granodiorite porphyry	Clay gouge (2% clay, PI = 17%)	0	26.5		
Granite	Clay filled faults Sandy loam fault filling Tectonic shear zone schistose and broken granites, disintegrated rock, and gouge	0-0.1 0.05 0.24	24-45 40 42		
Greywacke	1-2 mm clay in bedding planes			0	21
Limestone	6 mm clay layer 10-20 mm clay fillings <1 mm clay filling	0.1 0.05-0.2	13-14 17-21	0	13
Limestone, Marl, Lignites	Interbedded lignite layers Lignite/marl contact	0.08 0.1	38 10		
Limestone	Marlaceous joints, 20 mm thick	0	25	0	15-24
Lignite	Layer between lignite and clay	0.014-.03	15-17.5		
Montmorillonite Bentonite clay	80 mm seams of bentonite (montmorillonite) clay in chalk	0.36 0.016-.02	14 7.5-11.5	0.08	11
Schists, quartzites siliceous schists	100-15- mm thick clay filling Stratification, thin clay Stratification, thick clay	0.03-0.08 0.61-0.74 0.38	32 41 31		
Slates	Finely laminated and altered	0.05	33		
Quartz / kaolin / pyrolusite	Remoulded triaxial tests	0.042-.09	36-38		

Where a significant thickness of clay or gouge fillings occurs in rock masses and where the shear strength of the filled discontinuities is likely to play an important role in the stability of the rock mass, it is strongly recommended that samples of the filling be sent to a soil mechanics laboratory for testing.

Influence of water pressure

When water pressure is present in a rock mass, the surfaces of the discontinuities are forced apart and the normal stress σ_n is reduced. Under steady state conditions, where there is sufficient time for the water pressures in the rock mass to reach equilibrium, the reduced normal stress is defined by $\sigma_n' = (\sigma_n - u)$, where u is the water pressure. The reduced normal stress σ_n' is usually called the effective normal stress, which can be used in place of the normal stress term σ_n in all the equations presented above.

Instantaneous cohesion and friction

Due to the historical development of the subject of rock mechanics, many of the analyses, used to calculate factors of safety against sliding, are expressed in terms of the Mohr-Coulomb cohesion (c) and friction angle (ϕ), defined in Equation 1. Since the 1970s it has been recognised that the relationship between shear strength and normal stress is more accurately represented by a non-linear relationship such as that proposed by Barton and Bandis (1990). However, because this relationship is not expressed in terms of c and ϕ, it is necessary to devise some means for estimating the equivalent cohesive strengths and angles of friction from relationships such as those proposed by Barton and Bandis.

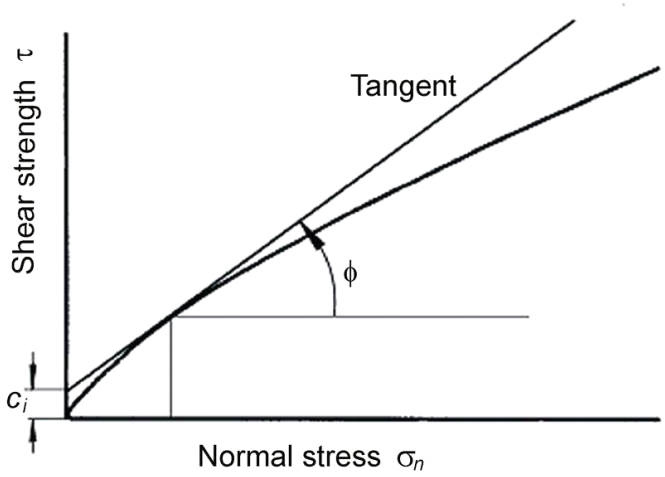

Figure 7: Definition of instantaneous cohesion c_i and the instantaneous friction angle ϕ_i for a non-linear failure criterion.

Figure 7 gives definitions of the *instantaneous cohesion* c_i and the *instantaneous friction* angle ϕ_i for a normal stress of σ_n. These quantities are given by the intercept and the inclination, respectively, of the tangent to the non-linear relationship between shear strength and normal stress. These quantities may be used for stability analyses in which the Mohr-Coulomb failure criterion (Equation 1) is applied, provided that the normal stress σ_n is reasonably close to the value used to define the tangent point.

Note that equation 4 is not valid for $\sigma_n = 0$ and it ceases to have any practical meaning for $\phi_r + JRC \log_{10}(JCS / \sigma_n) > 70°$. This limit can be used to determine a minimum value for σ_n. An upper limit for σ_n is given by σ_n = JCS.

In a typical practical application, a spreadsheet program can be used to solve equation 4 and to calculate the instantaneous cohesion and friction values for a range of normal stress values. In this spreadsheet the instantaneous friction angle ϕ_i, for a normal stress of σ_n, can be calculated from the relationship:

$$\phi_i = \arctan\left(\frac{\partial\tau}{\partial\sigma_n}\right) \tag{8}$$

$$\frac{\partial\tau}{\partial\sigma_n} = \tan\left(JRC\log_{10}\frac{JCS}{\sigma_n} + \phi_r\right) - \frac{\pi JRC}{180\ln 10}\left[\tan^2\left(JRC\log_{10}\frac{JCS}{\sigma_n} + \phi_r\right) + 1\right] \tag{9}$$

The instantaneous cohesion c_i is calculated from:

$$c_i = \tau - \sigma_n \tan\phi_i \tag{10}$$

In choosing the values of c_i and ϕ_i for use in a particular application, the average normal stress σ_n acting on the discontinuity planes should be estimated and used to determine the appropriate row in the spreadsheet. For many practical problems in the field, a single average value of σ_n will suffice but, where critical stability problems are being considered, this selection should be made for each important discontinuity surface.

References

Barton, N.R 1982. Modelling rock joint behaviour from in situ block tests: *Implications for Nuclear Waste Repository Design*. ONWI 308. Prepared by Tera Tek, Inc. for Office of Nuclear Waste Isolation, Battelle Memorial Institute, Columbus, Ohio.

Barton, N.R. 1974. *A review of the shear strength of filled discontinuities in rock.* Norwegian Geotech. Inst. Publ. No. 105. Oslo: Norwegian Geotech. Inst.

Barton, N.R. 1976. The shear strength of rock and rock joints. *Int. J. Mech. Min. Sci. & Geomech. Abstr*. **13**(10), 1-24.

Barton, N.R. and Bandis, S.C. 1982. Effects of block size on the shear behaviour of jointed rock. *23rd U.S. symp. on rock mechanics*, Berkeley, 739-760.

Barton, N.R. and Bandis, S.C. 1990. Review of predictive capabilities of JRC-JCS model in engineering practice. In *Rock joints, proc. int. symp. on rock joints,* Loen, Norway, (editors N. Barton and O. Stephansson), 603-610. Rotterdam: Balkema.

Barton, N.R. and Choubey, V. 1977. The shear strength of rock joints in theory and practice. *Rock Mech.* **10**(1-2), 1-54.

Hencher, S.R. & Richards, L.R. (1982). The basic frictional resistance of sheeting joints in Hong Kong granite *Hong Kong Engineer*, Feb., 21-25.

Patton, F.D. 1966. Multiple modes of shear failure in rock. *Proc. 1st congr. Int. Soc. Rock Mech.*, Lisbon **1**, 509-513.